Thermochimica Acta, 163 (1990) 279–286
Elsevier Science Publishers B.V., Amsterdam – Printed in The Netherlands

HEAT CAPACITY MEASUREMENT OF α-Ti-O SOLID SOLUTION DOPED WITH VANADIUM AND ALUMINIUM FROM 320 TO 910K

T. Tsuji, M. SATO and K. NAITO
Department of Nuclear Engineering, Faculty of Engineering,
Nagoya University, Furo-cho, Chikusa-ku, Nagoya 464-01 (Japan)

SUMMARY

Heat capacities of titanium-oxygen alloys, $TiO_{0.215}$, $TiO_{0.306}$, $TiO_{0.409}$ and $TiO_{0.466}$, and those of doped alloys, $(Ti_{1-y}V_y)_{\sim 0.2}$ (y=0.016 and 0.048) and $(Ti_{1-y}Al_y)O_{\sim 0.2}$ (y=0.03 and 0.05), were measured from 320 to 910K by adiabatic scanning calorimetry. Two kinds of heat capacity anomalies were observed for all samples except the O/Ti composition of 0.466. The anomaly at higher temperatures is assigned to be due to an order-disorder rearrangement of oxygen atoms. Another anomaly obtained at lower temperatures depends on cooling condition, indicating that this anomaly is due to a nonequilibrium phenomenon. The enthalpy and entropy changes due to the order-disorder transition for α-Ti-O solid solution obtained from this experiment are compared with theoretical values. The transition temperature, and enthalpy and entropy changes due to order-disorder transition decrease with increasing dopant contents of vanadium and aluminium, indicating that arrangement of oxygen atoms at lower temperatures may be partially ordered by the interaction between doped metal and oxygen atoms.

INTRODUCTION

Phase and crystallographic studies (refs. 1-7) on the titanium-oxygen alloys have shown that there are three phases, α, α' and α" for the O/Ti compositions, 0~0.4. In the α-phase at higher temperatures, the oxygen atoms dissolved in α-titanium metal are distributed randomly in octahedral sites of h.c.p. lattice. In the α'- and α"-phases of higher oxygen compositions and lower temperatures, the interstitial superstructures are formed in the primary solid solution of the titanium-oxygen system. The crystal structure of α'-phase is a layer-ordered structure (space group $P\bar{3}m1$, No.164) with the same unit cell as α-titanium (refs 1, 4-6). The completely ordered phase α" has a trigonal symmetry (space group $P\bar{3}1C$, No.163) with the cell dimension of $a=\sqrt{3}\ a_0$ and $c=2c_o$, where a_0 and c_o are the lattice constants of the original h.c.p. cell (refs. 2,5). The oxygen

0040-6031/90/$03.50

distribution in this phase is generally specified in terms of occupation probabilities for three octahedral interstitial sites.

Anomalies in various physical properties due to the order-disorder transition in titanium-oxygen alloys have been observed for the electrical conductivity measurement (refs. 8-10), magnetic susceptibility (refs. 8), X-ray photoemission spectrum (ref. 8), thermal expansion (ref. 11), static lattice distortion (ref. 12) and the diffusion coefficient of oxygen (ref. 13) as functions of temperature and the oxygen composition.

Koiwa and Hirabayashi (ref. 3) measured the heat capacity of α-Ti-O solid solution for the O/Ti compositions, 0.08~0.40 and found that the enthalpy and entropy changes measured for the transition were much smaller than those calculated on the basis of Bragg-Williams approximation (ref. 18).

In this paper, we measured the heat capacity of α-Ti-O solid solution doped with vanadium and aluminium from 320 to 910 K in order to clarify the transition mechanism from the transition temperatures, and transition enthalpy and entropy for the order-disorder transitions.

EXPERIMENTAL

Sample preparation

Samples of titanium-oxygen alloys with O/Ti ratio of 0.215, 0.306, 0.409 and 0.466 were prepared as follows; titanium metal sponge of 99.5 % purity and titanium dioxide powders of 99.99 % purity were mixed in an appropriate ratio and melted a few times using a plasma jet furnace under Ar gas stream. The cast sample obtained was sealed in a quartz tube, annealed one week at 1273 K, and cooled to room temperature over a period of 3 days. The sample was crushed into less than 3 mm in size using a stainless-steel mortar. The crushed sample of about 14 g was sealed in a quartz vessel filled with He gas of 20 kPa and then annealed at 573K for 1 week and cooled slowly to room temperature over a period of 1 week to obtain a highly ordered sample. X-ray diffractometry showed that $TiO_{0.215}$, $TiO_{0.306}$ and $TiO_{0.409}$ samples were α-Ti-O single phase, but $TiO_{0.466}$ was the mixture of α-Ti-O and TiO phases. The O/Ti ratio of the sample was determined from the weight gain by oxidizing it to TiO_2 in the temperature range from 1073 to 1273 K in air for 2 weeks.

Doped samples of $(Ti_{0.984}V_{0.016})O_{0.200}$, $(Ti_{0.952}V_{0.048})O_{0.200}$,

$(Ti_{0.97}Al_{0.03})O_{0.212}$ and $(Ti_{0.95}Al_{0.05})O_{0.215}$ were prepared by using similar method to undoped titanium-oxygen alloys. The V/Ti ratio of the sample was determined by fluorescent X-rays analysis. In the case of the sample doped with aluminium, the nominal composition was used because of the difficulty for detection of aluminium. X-ray diffractometry showed that all the samples except $(Ti_{0.952}V_{0.048})O_{0.200}$ were a single phase of α-Ti-M-O(M=V or Al) solid solution.

Heat capacity measurement

Heat capacities of α-Ti-O solid solution doped with vanadium and aluminium from 320 to 910K were measured by an adiabatic scanning calorimeter (ref. 14); in this calorimeter the power supplied to the sample was measured continuously, and the heating rate was kept constant regardless of the kind and amount of sample. The heating rate chosen was 2 K min^{-1}, and the measurement was carried out between 320 and 910K under a pressure of about 130 Pa of air. The heating rate and adiabatic control were usually maintained within ±0.005 K min^{-1} and ±0.01 K, respectively. The heat capacity measurement was conducted within an imprecision of ±1.5%.

RESULTS AND DISCUSSION

Heat capacity of α-Ti-O alloy

The results of the heat capacity measurement on $TiO_{0.215}$, $TiO_{0.306}$, $TiO_{0.409}$ and $TiO_{0.466}$ are shown in Fig. 1, where the baseline of heat capacity for each sample is calculated from Kopp-Neumann's rule by using heat capacities of Ti and TiO. As seen in the figure, the heat capacity data of $TiO_{0.466}$ are in good agreement with those of the baseline above 800K. It is also seen in the figure that a heat capacity anomaly due to order-disorder transition from the α"- to α-phase through the intermediate phase α' is observed especially for $TiO_{0.306}$ in the temperature range from 700 to 850K, and another broad peak is obtained around 300-600K below the order-disorder transition temperature.

Figure 2 shows the results of heat capacity measurement of the slowly cooled and quickly cooled $TiO_{0.215}$ sample. In the figure, the baseline of heat capacity is calculated from Kopp-Neumann's rule. Anomaly obtained at the lower temperatures depends on the cooling condition, indicating that this anomaly is due to a noneguilibrium phenomenon which was observed for substitutional

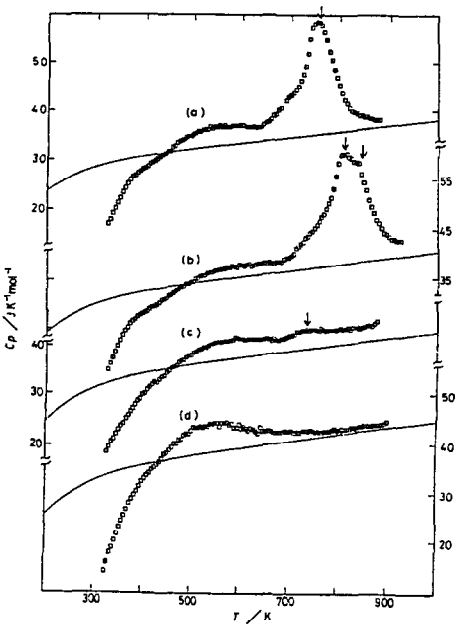

Fig. 1 Heat capacities of $TiO_{0.215}$ (a), $TiO_{0.306}$ (b), $TiO_{0.409}$ (c) and $TiO_{0.466}$ (d) from 320 to 910K. The baseline (solid line) of heat capacity for each sample is calculated from Kopp-Neumman's rule.

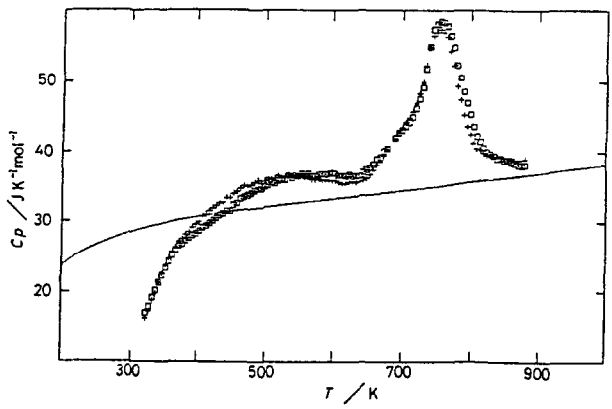

Fig. 2 Heat capacities of slowly (□) and quickly (+) cooled $TiO_{0.215}$. The baseline (solid line) of heat capacity is calculated from Kopp-Neumman's rule.

FeCo alloy quenched (refs. 15-17).

Figures 3 (a) and (b) show the configurational enthalpy and entropy changes of oxygens for $TiO_{0.215}$ sample which were

calculated from heat capacity data and the baseline shown in fig. 2 by using the following equations:

$$H(T) - H(880) = \int_{880}^{T} (Cp_1 - Cp_2)dT \quad (1)$$

and

$$S(T) - S(880) = \int_{880}^{T} \{(Cp_1 - Cp_2)/T\}dT \ , \quad (2)$$

where H(T) and H(880) are enthalpies at T and 880K, respectively, S(T) and S(880) entropies at T and 880K, respectively, Cp_1 and Cp_2 are heat capacity data measured in this study and those calculated from Kopp-Neumann's rule, respectively. It is assumed in this calculation that the partially (α') or completely disordered phases (α") are obtained at 880K. In the figure, the broken and dotted lines show a hypothetical equilibrium state, and slowly and quickly cooled ones, respectively. The configurational enthalpy and entropy changes for slowly cooled sample at room temperature are larger than those in equilibrium state due to freezing of oxygen movement at certain temperature. These higher configurational enthalpy and entropy changes at room temperature decrease with increasing temperature due to the movement of oxygen atoms to equilibrium state and then increase with increasing temperature to attain equilibrium state (the broken line). After the equilibrium, the configurational enthalpy and entropy changes increase with increasing temperature due to order-disorder transition based on the rearrangement of oxygen atoms. After the first run, the sample is cooled in the calorimeter along the path shown by the dotted line (quickly cooled) and then quickly cooled configurational enthalpy and entropy data were obtained as shown in figs. 3 (a) and (b). Thus, the configurational enthalpy and entropy changes for quickly cooled sample are larger than those

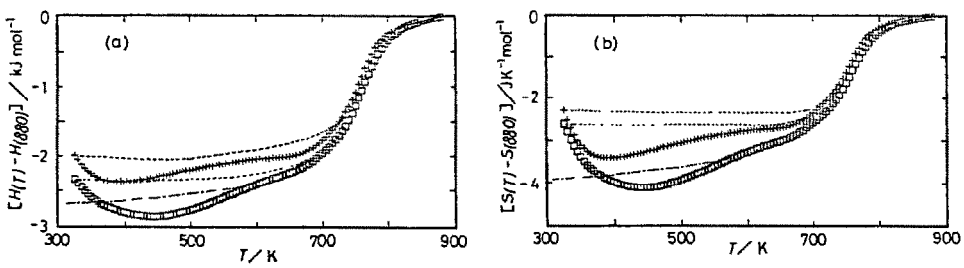

Fig. 3 Plots of configurational enthalpy (a) and entropy (b) changes against T for slowly (□) and quickly (+) cooled $TiO_{0.215}$.
—·— hypothetical equilibrium state,
------ hypothetical slowly and quickly cooled states.

for slowly cooled one as the sample is quenched in higher degree of regularity. These phenomena are considered to be related to the movement of oxygen atoms. Although it is difficult to get configurational enthalpy and entropy changes exactly due to the contribution of non-equilibrium data, these values may be obtained from the difference between the maximum and minimum of each sample shown in figs. 3 (a) and (b).

Figure 4 shows the transition enthalpy and entropy calculated from fig. 1 by using eqs. (1) and (2), together with the transition temperature (peak temperature of heat capacity shown in fig. 1) as a function of O/Ti ratio. In fig. 4, $dH_1(S_1)$ and $dH_1+dH_2(dS_1+dS_2)$ are the theoretical transition enthalpy (entropy) due to the order-disorder transition of oxygen atoms in the intra-plane (from α"- to α'-phase) and that of both intra- and inter-planes (from α"- to α-phase), respectively (ref. 18). The transition temperatures of each sample in this study are in good agreement with those by Koiwa and Hirabayashi (ref. 3) as seen in fig. 4. The transition enthalpy and entropy from the completely

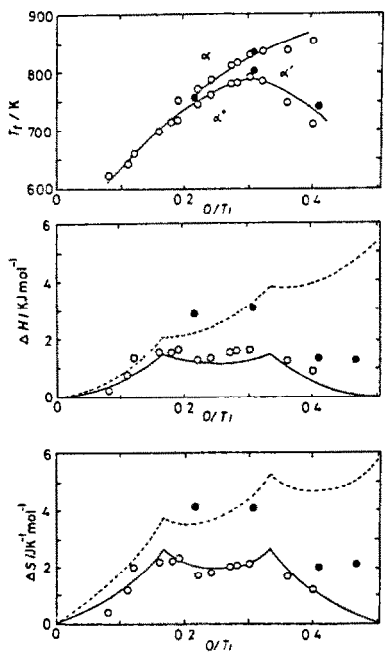

Fig. 4 Plots of transition temperature (T_t), and transition enthalpy (ΔH) and entropy (ΔS) due to order-disorder transition against the O/Ti ratio. —— dS_1, ------ dS_1+dS_2, ●: this work, o: Koiwa and Hirabayashi (ref. 3).

ordered phase (α") to completely disorderd phase (α) for $TiO_{0.215}$ and $TiO_{0.306}$ samples in this experiment are larger than those by Koiwa and Hirabayashi (ref. 3) and are in good agreement with their theoretical values (ref. 18). On the other hand, the transition enthalpy and entropy by the present author are smaller than the theoretical values for $TiO_{0.409}$ and $TiO_{0.466}$ samples, indicating that some modifications of the theoretical model by Koiwa and Hirabayashi may be needed to explain the order-disorder transition at higher oxygen compositions.

HEAT CAPACITY OF α-$(Ti_{1-y}V_y)O_x$ AND α-$(Ti_{1-y}Al_y)O_x$

Heat capacities of $(Ti_{1-y}V_y)O_{\sim 0.2}$ (y=0, 0.016 and 0.048) and $(Ti_{1-y}Al_y)O_{\sim 0.2}$ (y=0, 0.03 and 0.05) in the temperature range from 320 to 910K are shown in figs. 5 (a) and (b), respectively. As seen in figs. 5 (a) and (b), heat capacities of doped

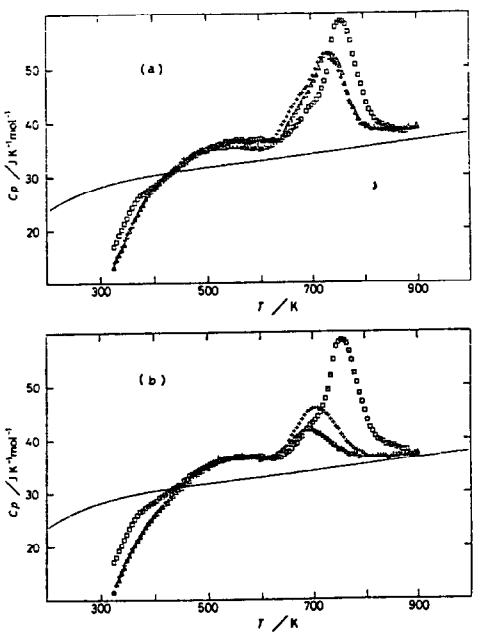

Fig. 5 Heat capacities of α-Ti-M-O (M=V or Al) solid solution. (a) $(Ti_{1-y}V_y)O_{\sim 0.2}$ (y=0(□), 0.016(+) and 0.048(△)). (b) $(Ti_{1-y}Al_y)O_{\sim 0.2}$ (y=0 (□), 0.03(+) and 0.05(△)).

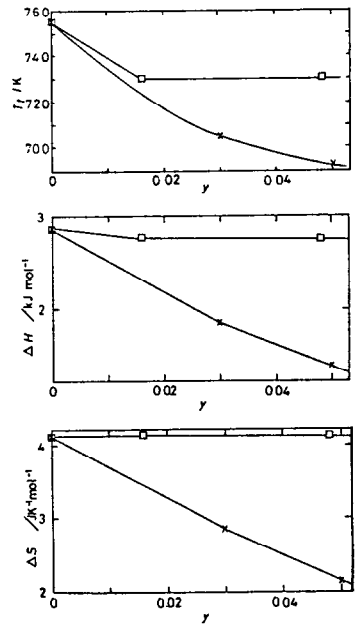

Fig. 6 Transition temperature (T_t), and transition enthalpy (ΔH) and entropy (ΔS) due to order-disorder transition as a function of y for $(Ti_{1-y}M_y)_{\sim 0.2}$ (M=V or Al). □——□ doped with V, ×——× doped with Al.

$(Ti_{1-y}V_y)O_{\sim 0.2}$ and $(Ti_{1-y}Al_y)O_{\sim 0.2}$ at 320K are smaller than that of undoped $TiO_{0.2}$ sample, and both values agree in the temperature range from 450 to 600K. It is also seen that the transition temperature and peak area of heat capacity due to order-disorder transition at high temperature decrease with increasing dopant contents of vanadium and aluminium. However, both heat capacity data of $(Ti_{1-y}V_y)O_{\sim 0.2}$ (y=0.016 and 0.048) are not different each other, because the solubility limit of vanadium is less than 4.8 at% as expected from X-ray diffractometry. The transition temperature, and transition enthalpy and entropy of doped samples are plotted in fig. 6 as a function of dopant contents. As seen in the figure, the transition temperature, and transition enthalpy and entropy decrease with increasing dopant contents and the doped effect of aluminium is larger than that of vanadium. These facts may be explained by the decrease of regularity due to the interaction between doped metal and oxygen atoms.

REFERENCES

1 B. Holmberg, Acta Chem. Scand. 16 (1962) 1245-1250.
2 S. Yamaguchi, M. Koiwa and M. Hirabayashi, J. Phys. Soc. Japan 21 (1966) 2096.
3 M. Koiwa and M. Hirabayashi, J. Phys. Soc. Japan, 27 (1969) 801-806.
4 S. Yamaguchi, J. Phys. Soc. Japan 27 (1969) 155-163.
5 S. Yamaguchi, K. Hiraga and M. Hirabayashi, J. Phys. Soc. Japan 28 (1970) 1014-1023.
6 S. Andersson, B. Collén, U. Kuylenstierna and A. Magnéli, Acta Chem. Scand. 11 (1957) 1641-1652.
7 T. Arai and M. Hirabayashi, J. Phys. Soc. Japan 42 (1977) 1965-1971.
8 T. Arai and M. Hirabayashi, J. Phys. Soc. Japan 41 (1976) 1239-1246.
9 H. Gruber and E. Krantz, Phys. Stat. Sol. 69a (1982) 287-295.
10 A. Filion, J. P. Nérou and P-E Girard, J. Phys. F: Metal Phys., 5 (1975) 468-479.
11 R. J. Wasilewski, Trans. Met. Soc. AIME, 221 (1961) 1231-1235.
12 F. R. L. Schoening and F. Witt, Acta Cryst. 18 (1965) 609-614.
13 D. David, G. Beranger and E. A. Garcia, J. Electrochem. Soc. 130 (1983) 1423-1426.
14 K. Naito, H. Inaba, M. Ishida, Y. Saito and H. Arima, J. Phys. E 7 (1974) 464-468.
15 H. Sato and R. Kikuchi, Acta Metall., 24 (1976) 797-809.
16 K. Gschwend, H. Sato and R. Kikuchi, J. Chem. Phys., 69 (1978) 5006-5019.
17 K. Gschwend, H. Sato, R. Kikuchi, H. Iwasaki and H. Maniwa, J. Chem. Phys., 71 (1979) 2844-2852.
18 M. Koiwa and M. Hirabayashi, J. Phys. Soc. Japan, 27 (1969) 807-815.